

Article

Novel Tunable Green-Red Luminescence in Mn^{2+} Doped $\text{Ca}_9\text{Tb}(\text{PO}_4)_7$ Phosphors Based on the Mn^{2+} Regulation and Energy Transfer

Bingwen Yang ¹, Yefeng Feng ¹, Qinghu Zhao ¹, Miao He ^{1,*} and Yang Lv ^{2,*}

¹ School of Physics and Optoelectronic Engineering, Guangdong University of Technology, WaiHuan Xi Road, No. 100, Guangzhou 510006, China; 1111715003@mail2.gdut.edu.cn (B.Y.); fengyefeng_1001@163.com (Y.F.); ybwowem1@163.com (Q.Z.)

² College of Mathematics and Systems Science, School of Optoelectronic Engineering, No. 293, Zhongshan Avenue West, Tianhe District, Guangzhou 510665, China

* Correspondence: hemiao1600@163.com (M.H.); lvyang@gpnu.edu.cn (Y.L.)

Received: 10 September 2020; Accepted: 29 September 2020; Published: 1 October 2020



Abstract: $\beta\text{-Ca}_3(\text{PO}_4)_2$ type phosphors $\text{Ca}_9\text{Tb}(\text{PO}_4)_7:\text{Mn}^{2+}$ were fabricated by high temperature solid state reaction. Under 377 nm light excitation, the $\text{Ca}_9\text{Tb}(\text{PO}_4)_7$ host displays the green emission attributable to the characteristic emission of Tb^{3+} ions peaking at 488, 542, 586, and 620 nm, respectively. The red broadband emission is observed when $\text{Ca}_9\text{Tb}(\text{PO}_4)_7$ is doped with Mn^{2+} ions. The emission is attributed to the energy transfer from Tb^{3+} to Mn^{2+} ions; this facilitates the realization of the tunable green–red emission. The energy transfer mechanism from Tb^{3+} to Mn^{2+} is defined as quadrupole–quadrupole interaction. Furthermore, the thermal stability of $\text{Ca}_9\text{Tb}(\text{PO}_4)_7:\text{Mn}^{2+}$ samples has been studied, and it can maintain half the emission intensity exceeding 424 K. This demonstrates their potential applications in white light LEDs (w-LEDs).

Keywords: high thermal stability; $\beta\text{-Ca}_3(\text{PO}_4)_2$; tunable emission

1. Introduction

Phosphate-based phosphors can form various crystal field environments that impose on the emitting center [1]. $\beta\text{-Ca}_3(\text{PO}_4)_2$ and its derivatives are important compounds that have been widely researched for use in white light LEDs (w-LEDs), temperature sensing and plasma display panels. Their advantages include high luminescent efficiency, as well as good physical and chemical stability. Recently, researchers have developed numerous single-component phosphate phosphors with tunable color emission and white light emission that can be used in UV-excited w-LEDs which have been developed by researchers, such as $\text{Sr}_9\text{Mg}_{1.5}(\text{PO}_4)_7:\text{Eu}^{2+}$, $(\text{Ca},\text{Sr})_9(\text{PO}_4)_7:\text{Eu}^{2+}/\text{Mn}^{2+}$, $\text{Ca}_2\text{Sr}(\text{PO}_4)_2:\text{Eu}^{2+}/\text{Mn}^{2+}$, $\text{Ca}_9\text{Bi}(\text{PO}_4)_7:\text{Ce}^{3+}/\text{Tb}^{3+}/\text{Mn}^{2+}$, $\text{Ca}_8\text{MgLu}(\text{PO}_4)_7:\text{Ce}^{3+}/\text{Tb}^{3+}/\text{Mn}^{2+}$, $(\text{Ca},\text{Mg},\text{Sr})_9(\text{PO}_4)_7:\text{Eu}^{2+}/\text{Mn}^{2+}$ and $\text{Ca}_{9-x-y-z}\text{Mg}_x\text{Sr}_y\text{Ba}_z\text{Ce}(\text{PO}_4)_7:\text{Eu}^{2+}/\text{Mn}^{2+}$ [2–8]. Furthermore, $\beta\text{-Ca}_3(\text{PO}_4)_2$ and its derivatives have garnered interest for application in temperature sensing, owing to the excellent thermal stability of Mn^{2+} emission which originates from the energy compensation of stored electrons [9,10]. To manufacture an efficient solid-state lighting equipment, it is crucial for the phosphors to possess the following characteristics: adjustable emission color to regulate the ratio of each color in the spectra, environmental friendliness, and appreciable thermal stability to maintain increased luminous efficiency at high temperature.

Phosphors doped with Mn^{2+} have exhibited a broad emission band ranging from 500 to 700 nm, which is determined by the matrix crystal field. Green emission is usually displayed in weak crystal fields (tetrahedrally coordinated sites) and red emission is demonstrated in strong crystal fields (octahedral coordinated sites) [11–13]. In addition, the Mn^{2+} ion usually exhibits red emission in $\text{Ca}_9\text{Ln}(\text{PO}_4)_7$ structure compounds. However, the absorption and emission bands of

Mn^{2+} d–d are relatively weak because of their parity and spin confinement transitions. Therefore, it is necessary to enhance their emission intensity via energy transfer using sensitizers like Ce^{3+} , Tb^{3+} , Eu^{2+} ions. Moreover, the efficient sensitization of Mn^{2+} emission and tunable color should be realized, for example, $\text{Ca}_8\text{BaCe}(\text{PO}_4)_7:\text{Tb}^{3+}/\text{Mn}^{2+}$, $\text{Ca}_9\text{Y}(\text{PO}_4)_7:\text{Ce}^{3+}/\text{Mn}^{2+}$, $\text{Ca}_9\text{Ce}(\text{PO}_4)_7:\text{Eu}^{2+}/\text{Mn}^{2+}$ and $0.1\text{Ca}_9\text{Y}(\text{PO}_4)_7-0.9\text{Ca}_{10-z}\text{Na}_{1+z}(\text{PO}_4)_7:\text{Eu}^{2+},\text{Mn}^{2+}$ [3,4,10,14–16]. However, the Ce^{3+} and Eu^{2+} ions are typically formed in a reducing atmosphere, and the Tb^{3+} ions are formed in an air atmosphere with a lower, more stable consumption. In addition, Tb^{3+} ions have previously been used as one of the matrix ions, and as a sensitizer to enhance the red emission [17,18]. A series of the whitlockite structure $\text{Ca}_9\text{Ln}(\text{PO}_4)_7$ (Ln = lanthanide) materials with matrix luminescence originating from the $\beta\text{-Ca}_3(\text{PO}_4)_2$ derivants are receiving increasing interest in this field of research [19]. In this $\text{Ca}_9\text{Ln}(\text{PO}_4)_7$ group, Ln includes all the non-radioactive rare earth (Eu, Ho, Tb, Dy, Pr, Sm, Yb, Nd, Er and Tm) elements. These matrix materials exhibit the characteristic emission of Ln ions. Therefore, the possibility of using Tb^{3+} ions as sensitizers to improve the luminescence properties of Mn^{2+} in the whitlockite structure can be considered. Based on this, it can be concluded that $\text{Ca}_9\text{Tb}(\text{PO}_4)_7$ (CTP) will be an important candidate for strengthening the Mn^{2+} emission.

In this study, we have reported green–red tunable color Mn^{2+} -doped CTP phosphors synthesized via high-temperature solid method. The CTP host displays a characteristic green emission of Tb^{3+} ion upon 377 nm light excitation. In addition, the red emission is observed while Mn^{2+} doped into CTP, owing to the energy transfer from Tb^{3+} to Mn^{2+} ions. Additionally, the fluorescence lifetimes have been studied systematically. The Mn^{2+} emission reaches the maximum at $x = 0.3$, and then monotonically decreases with an increase in the Mn^{2+} concentrations, owing to the concentration quenching. Besides, the thermal stability of the phosphors CTP: Mn^{2+} phosphors we prepared has been researched: they can maintain half the strength even at temperatures above 424 K, indicating that these whitlockite structure phosphors have promising applications in w-LEDs.

2. Experimental

2.1. Materials and Synthesis

Whitlockite structure luminescent materials of CTP: Mn^{2+} were synthesized by high-temperature solid-state method. The raw materials were CaCO_3 (99.7%), Tb_4O_7 (99.99%), $(\text{NH}_4)_2\text{HPO}_4$ (99.7%) and MnCO_3 (99.7%), and they were weighed according to the stoichiometric ratio of $\text{Ca}_{9-x}\text{Tb}(\text{PO}_4)_7:x\text{Mn}^{2+}$ ($x = 0.05, 0.1, 0.2, 0.3, 0.4, 0.5, 0.6, 0.7$), ground thoroughly, and mixed in an agate mortar and ground thoroughly to obtain the mixtures. Firstly, the mixtures were pre-sintered in a tube furnace at 500 °C for 2 h. The intermediate products were then reground thoroughly and transferred to a high-temperature tube furnace, sintered at 1200 °C for 4 h in the ambient atmosphere. Finally, the obtained products were ground to a fine powders for the following measurements.

2.2. Characterization

The X-ray diffraction (XRD) patterns were performed on a D8 ADVANCE X-ray diffractometer (Bruker, Billerica, MA, USA) with $\text{Cu K}\alpha$ irradiation ($\lambda = 1.5406$ nm). Photoluminescence excitation (PLE) and photoluminescence (PL) spectra were collected on an Edinburgh FLS 980 Fluorescence Spectrophotometer (Edinburgh Instruments, Edinburgh, Britain). The temperature-dependent PL spectra were also measured on the Edinburgh FLS 980 Fluorescence Spectrophotometer equipped with the variable temperature accessories. SEM images were characterized using a scanning electron microscope (Sipra 55 Sapphire, Zeiss, Oberkochen, German), and the elemental mapping was collected via EDX spectroscopy (Oxford X-max 20, Oxford, London, UK).

3. Results and Discussion

3.1. Phase Characterization and SEM Analysis

The phase purity of the CTP:Mn²⁺ samples was verified using XRD measurements; the representative XRD patterns are shown in Figure 1. Ca₉Tb(PO₄)₇ can not be found in the Joint Committee on Powder Diffraction Standards (JCPDS); however, the obtained samples are indexed to the JCPDS data PDF#46-0402 (Ca₉Y(PO₄)₇), demonstrating that the obtained phosphors are crystallized in a single phase. There is no any clear impure phase that occurs after the Mn²⁺ ion was doped into the CTP host. These results demonstrate that Mn²⁺ ion doping can preserve the crystal structure. The CTP host has three types of Ca²⁺ ions positions with six-fold, eight-fold and nine-fold coordination, respectively.

In addition, Figure 1b indicates that certain diffraction peaks move towards a large angle direction while the content of Mn²⁺ ions increase. This movement can be attributed to the Mn²⁺ ions doping. Based on the charge balance and effective ionic radius, the Ca²⁺ ion (1.00 Å, coordination (CN) = 6; 1.12 Å, CN = 8; 1.18 Å, CN = 9), Mn²⁺ ion (0.83 Å, CN = 6; 0.96 Å, CN = 8), we suggest the simultaneous substitution of Ca²⁺ ions with Mn²⁺ ions at three sites. Therefore, the shift of the diffraction peaks to a larger angle direction can be interpreted by the Bragg's equation $2d \times \sin\theta = n\lambda$, when the Mn²⁺ ions with a smaller radius replace the Ca²⁺ ions with a larger radius.

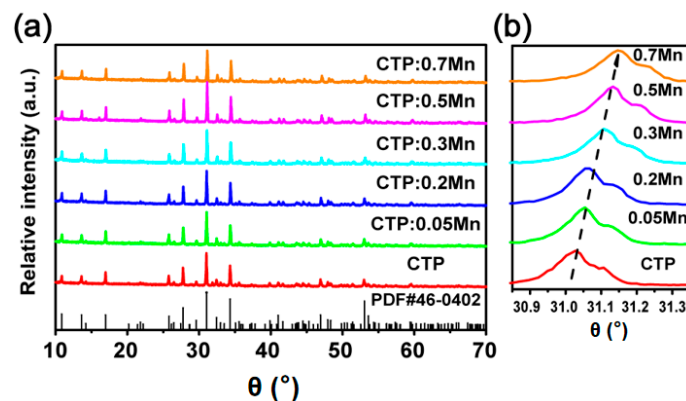


Figure 1. (a) Typically XRD patterns of CTP:*x*Mn²⁺ together with the standard data, (b) The XRD patterns ranging from 30.8 to 31.4°.

The SEM images and EDS element mapping for the morphology investigations of the CTP:Mn²⁺ phosphor are shown in Figure 2. The CTP:Mn²⁺ phosphor displays appreciable crystallinity and the crystal shape is irregular with an approximate size of 10 μm. The element mapping images exhibit the uniform distribution of Ca, Tb, P, O, and Mn on the as-prepared phosphor, demonstrating that the Mn²⁺ ion was successfully doped into the CTP matrix.

3.2. Luminescence Performance and Energy Transfer of CTP:Mn²⁺ Phosphor

The PL and PLE spectra of CTP host are shown in Figure 3. It is evident from a series of peaks that the Tb³⁺ ions are effectively excited, displaying how the different relative intensity obtained the maximum value under 377 nm light excitation. The intense green light peaking at 488, 542, 586, 620 nm are attributed to the transition from the ⁵D₄ level to ⁷F₆, ⁷F₅, ⁷F₄ and ⁷F₃ level, respectively [20–23]. Monitoring at 542 nm, the PLE spectrum shows a series of narrow 4f–4f transition lines of Tb³⁺ in the range of 300–400 nm, which is ascribed to the electron transition from lower energy level ⁷F₆ to the excited level including ⁵H₇ (316 nm), ⁵L₆ (340 nm), ⁵G₄ (351 nm), ⁵L₉ (358 nm), ⁵D₂ (367 nm), ⁵D₃ (377 nm), and ⁵D₄ (482 nm) levels, respectively [17,24,25].

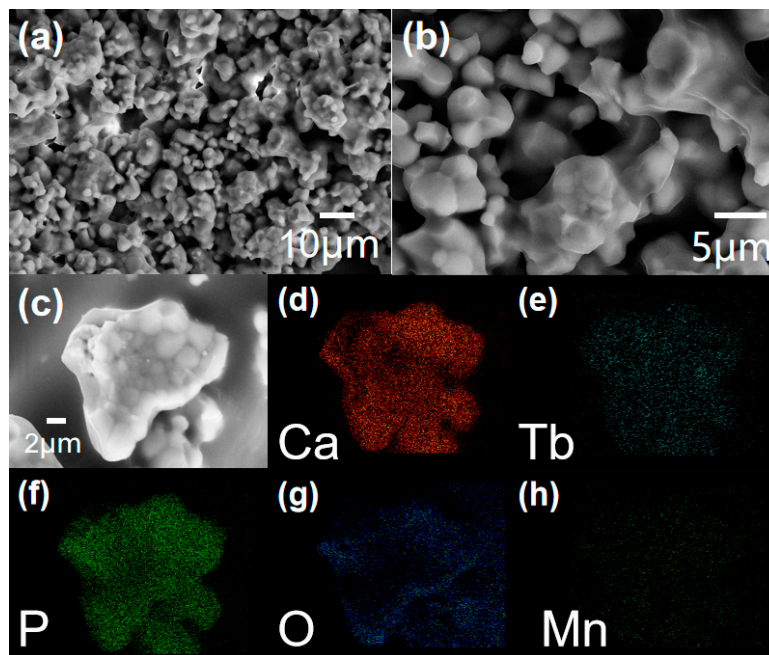


Figure 2. CTP:0.3Mn²⁺ phosphor SEM image of (a) 10 μm multiplying power, (b) 5 μm multiplying power, (c) 2 μm multiplying power, and EDS mapping of element, (d) Ca, (e) Tb, (f) P, (g) O, (h) Mn.

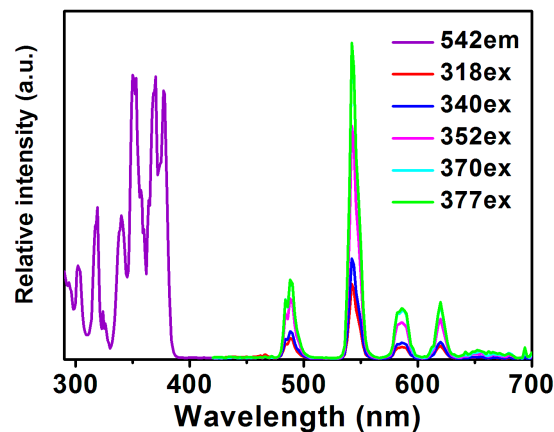


Figure 3. Photoluminescence excitation (PLE) and photoluminescence (PL) spectra of the CTP host.

Red emission is observed after the Mn²⁺ ion was doped into the CTP host, which is ascribed to the ⁴T₁(4G)→⁶A₁(6S) transition of the Mn²⁺ ions, as shown in Figure 4a. The green emission clearly decreases as the Mn²⁺ ion concentration increases, which could be ascribed to the energy transfer from sensitizer (Tb³⁺) to activator (Mn²⁺). In addition, the red emission of Mn²⁺ ions initially increases and reaches its maximum when the Mn²⁺ content is fixed at 0.3, then starts to decrease owing to the concentration quenching as the concentration continues to increase. Green–red tunable color is realized with the Mn²⁺ content increasing in the CTP host—the corresponding Commission Internationale de l’Eclairage (CIE) coordinate diagram and photographs are shown in Figure 4b. Furthermore, the energy transfer diagram from Tb³⁺ to Mn²⁺ ions in the CTP host is illustrated in Figure 5.

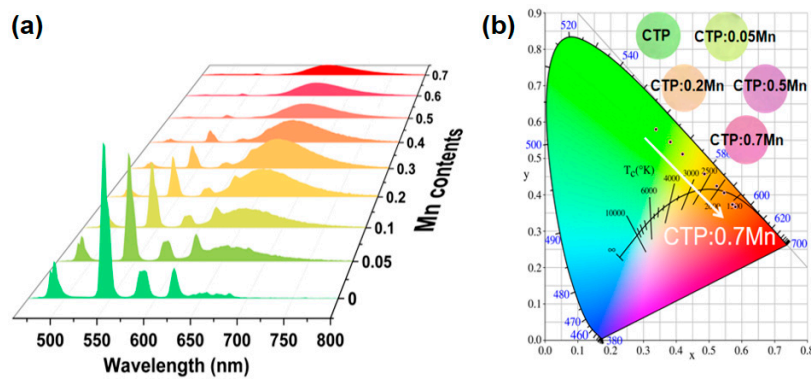


Figure 4. (a) PL spectra of CTP:*x*Mn²⁺ (*x* = 0.05, 0.1, 0.2, 0.3, 0.4, 0.5, 0.6 and 0.7), and (b) CIE coordinate diagram and representative photographs.

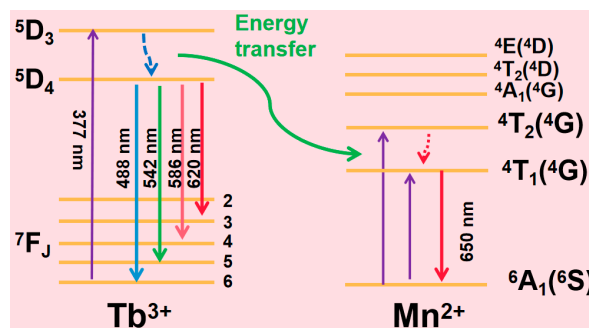


Figure 5. Energy-transfer mechanism for Tb³⁺ to Mn²⁺ in the CTP matrix.

To explain the energy transfer from Tb³⁺ to Mn²⁺ ions, the fluorescence lifetime of CTP:*x*Mn²⁺ (*x* = 0.05, 0.1, 0.2, 0.3, 0.4, 0.5, 0.6 and 0.7) is indicated in Figure 6a. The fluorescence lifetime of the CTP matrix can be fitted using the monoexponential decay function [26,27]:

$$I(t) = A \exp(-t/\tau) \tag{1}$$

where *I*(*t*) is the PL intensity of the Tb³⁺ ion at *t* time, *A* is the constant, *t* stands for the time and τ is the decay time of Tb³⁺ ion. The decay time of the Tb³⁺ ions will gradually decrease with an increase in Mn²⁺ ions, then this decay process can be expressed as the average lifetime, calculated by using the following function:

$$\tau = \frac{\int_0^\infty I(t)t dt}{\int_0^\infty I(t) dt} \tag{2}$$

The average lifetimes of Tb³⁺ ions with doping concentrations of Mn²⁺ ions are calculated to be 2.15, 1.81, 1.54, 1.29, 1.04, 0.98, 0.60, 0.14 and 0.08 ms at *x* = 0, 0.05, 0.1, 0.2, 0.3, 0.4, 0.5, 0.6 and 0.7, respectively. Hence, the estimated average lifetimes clearly explain the energy transfer from the Tb³⁺ to Mn²⁺ ion, which is consistent with the reduction in the PL intensity of Tb³⁺ ions. The following function is used to estimate the energy transfer efficiency [7,9,17]:

$$\eta = 1 - \tau/\tau_0 \tag{3}$$

where τ_0 and τ stand for the lifetimes of the Tb³⁺ ions without and with Mn²⁺ ions, respectively. The calculated energy transfer efficiencies are depicted in Figure 6b. In addition, the efficiency of energy transfer monotonically increases with the increase in Mn²⁺ ions content, reaching 96.3% at *x* = 0.7.

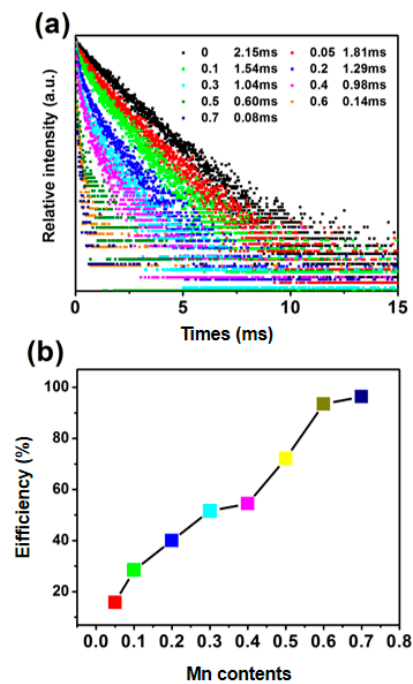


Figure 6. (a) Fluorescence lifetime of the Tb^{3+} ion with different Mn^{2+} contents in the $CTP:xMn^{2+}$ ($x = 0.05, 0.1, 0.2, 0.3, 0.4, 0.5, 0.6$ and 0.7) ($\lambda_{ex} = 377$ nm, $\lambda_{em} = 542$ nm); and (b) the energy transfer efficiency of $CTP:xMn^{2+}$ ($x = 0.05, 0.1, 0.2, 0.3, 0.4, 0.5, 0.6$ and 0.7).

Time-resolved spectra are typically employed to explicitly identify the luminescent centers in luminous systems [28,29]. The time-resolved spectroscopy of the sample $CTP:0.1Mn^{2+}$ is determined for the further verification of energy transfer from the Tb^{3+} to Mn^{2+} ion in the CTP host, as shown in Figure 7a. Two emission bands that belong to Tb^{3+} and Mn^{2+} ions are clearly observed, and the relative intensity between the Tb^{3+} and Mn^{2+} ions decreases with an increase in the decay times increasing as depicted in Figure 7b. In addition, the intensity of Tb^{3+} ions remains unchanged after 10 ms, and the intensity of Mn^{2+} ions is persisting to reduce over time, indicating that the energy is gradually transferred from Tb^{3+} to the Mn^{2+} ions and the energy transfer process is completed after 10 ms. These results establish the energy transfer from Tb^{3+} to Mn^{2+} ions.

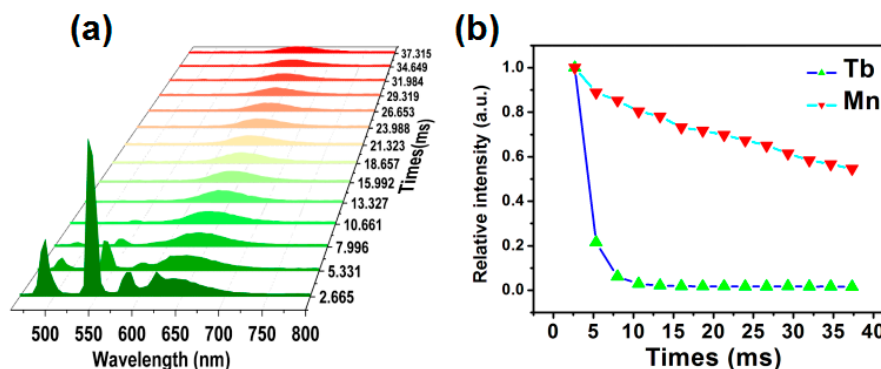


Figure 7. (a) Time-resolved spectroscopy of sample the $CTP:0.1Mn^{2+}$; and (b) the change in the trend of relative intensity of Tb^{3+} and Mn^{2+} over come.

Generally, the exchange interaction and electric multipole multipole interaction can lead to a nonradiative energy transfer between the sensitizer and activator [2–8,10,14–16]. If the exchange

is the reason for energy transfer, the emission intensity of Mn^{2+} ions will exhibit the following relationship [30,31]:

$$\ln(I_0/I) \propto C \quad (4)$$

where I_0 and I represent the emission intensity of the Tb^{3+} ions in the absence and presence of Mn^{2+} ions, respectively. C is the total contents of Tb^{3+} and Mn^{2+} ions in the CTP matrix. If electric multipole–multipole interaction is the primary cause of energy transfer from Tb^{3+} to Mn^{2+} ions, the emission intensity of Mn^{2+} ions will be determined using the following function:

$$\ln(I_0/I) \propto \ln C \quad (5)$$

the slope of the function is $\alpha/3$, where α equals to 6, 8, 10 which stand for dipole–dipole, dipole–quadrupole and quadrupole–quadrupole interactions, respectively. Thus, the relationships of $\ln(I_0/I)$ and $\ln C$ are depicted in Figure 8. It could be observed that the slope of linear fitting curve is 3.2974 in Figure 8, thus, the α is close to 10. This result illustrates that the energy transmission between the Tb^{3+} and Mn^{2+} ion is mainly caused by quadrupole–quadrupole interaction.

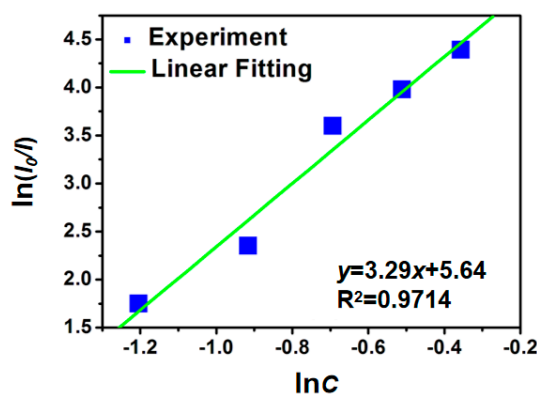


Figure 8. The dependence of $\ln(I_0/I)$ on $\ln C$ in the CTP: $x\text{Mn}^{2+}$ phosphors.

3.3. Temperature-Dependent PL Performance of CTP: Mn^{2+} Phosphor

Thermal stability is one significant factor for phosphors adopted in w-LEDs [32,33]. Normally, the emission intensity of phosphors should be maintained at a temperature above 423 K (150 °C) because the light-emitting diodes generate heat for long durations of time. Typically, the emission intensity monotonically decreases with an increase in temperature, and displays lower luminous efficiency. A series of phosphors with good thermal stability have been reported in recent years [10,34–36]. To investigate the thermal stability of a CTP: Mn^{2+} phosphor, the temperature-dependent (303 to 573 K) PL spectra of the CTP:0.3 Mn^{2+} phosphor was collected, as shown in Figure 9a. It can be easily observed that the emission intensity can maintain a half level even with a temperature up to 424 K.

To further study the thermal stability of the CTP: Mn^{2+} phosphor, the corresponding PL intensity of Tb^{3+} and Mn^{2+} ions for each temperature points are depicted in Figure 9b. Significantly, the CTP:0.3 Mn^{2+} phosphor we obtained has maintained the half emission intensity at 424 K, a result which demonstrates the good thermal stability for the CTP: Mn^{2+} phosphor. The relationship of $\ln(I_0/I-1)$ on $1/kT$ of the CTP:0.3 Mn^{2+} phosphor is shown in Figure 10, and the value of activation energy (E_a) is defined as 0.1846 eV. In conclusion, the as-prepared tunable green–red CTP: Mn^{2+} phosphors have promising application in w-LEDs.

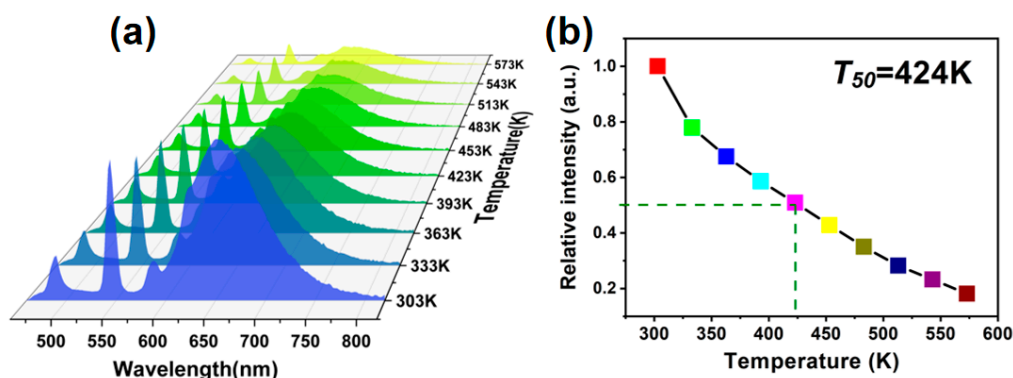


Figure 9. (a) Temperature-dependent PL spectra of the CTP:0.3Mn²⁺ phosphors ranging from 303 to 573 K; and (b) the variation tendency of Tb³⁺ and Mn²⁺ ions from 303 to 573 K.

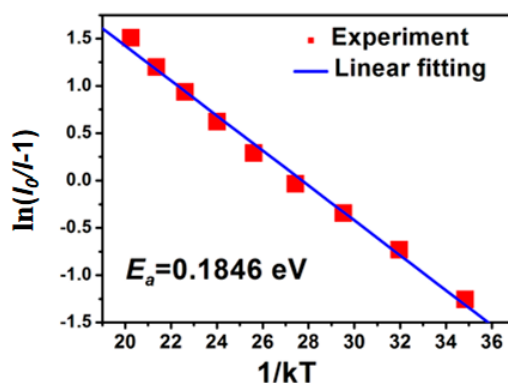


Figure 10. The relationship of the $\ln(I_0/I-1)$ versus $1/kT$ for the CTP:0.3Mn²⁺ phosphor.

4. Conclusions

In sum, the color-tunable green-red Mn²⁺ doped Ca₉Tb(PO₄)₇ phosphors have synthesized via traditional solid phase method. Under 377 nm light excitation, the Ca₉Tb(PO₄)₇ matrix shows green emission with several peaks belonging to the transition from ⁵D₄ level to ⁷F₆, ⁷F₅, ⁷F₄ and ⁷F₃ level, respectively. Red emission is clearly observed as the Mn²⁺ ions doping into Ca₉Tb(PO₄)₇. Color-tuning from green to red is realized by varying the Mn²⁺ contents. The sensitization of Tb³⁺ to Mn²⁺ renders the energy transfer from Tb³⁺ to Mn²⁺ ions effectively. The energy transmission efficiency reaches a maximum of 96.3% at $x = 0.7$. In addition, the theoretical mechanism for energy transmission from Tb³⁺ to Mn²⁺ ions has been investigated, and it is found to be dominated by the quadrupole-quadrupole interaction. Meanwhile, the Ca₉Tb(PO₄)₇:Mn²⁺ phosphor indicates good thermal stability, maintained the approximately half emission level at 424 K (150 °C), which demonstrates that the Ca₉Tb(PO₄)₇:Mn²⁺ phosphor can be potentially applied to w-LEDs.

Author Contributions: Conceptualization, B.Y. and Y.L.; methodology, B.Y.; software, B.Y.; validation, Q.Z., B.Y. and Y.F.; formal analysis, B.Y.; investigation, B.Y.; resources, Q.Z.; data curation, B.Y.; writing—original draft preparation, Y.L.; writing—review and editing, Y.L.; visualization, Y.F.; supervision, B.Y.; project administration, M.H.; funding acquisition, M.H. All authors have read and agreed to the published version of the manuscript.

Funding: This research was supported by the National Natural Science Foundation of China (NSFC) (61875187).

Conflicts of Interest: The authors declare no conflict of interest.

References

1. Song, H.J.; Yim, D.K.; Cho, I.-S.; Roh, H.-S.; Kim, J.S.; Kim, D.-W.; Hong, K.S. Luminescent properties of phosphor converted LED using an orange-emitting $\text{Rb}_2\text{CaP}_2\text{O}_7:\text{Eu}^{2+}$ phosphor. *Mater. Res. Bull.* **2012**, *47*, 4522–4526. [[CrossRef](#)]
2. Sun, W.; Jia, Y.; Pang, R.; Li, H.; Ma, T.; Li, D.; Fu, J.; Zhang, S.; Jiang, L.; Li, C. $\text{Sr}_9\text{Mg}_{1.5}(\text{PO}_4)_7:\text{Eu}^{2+}$: A novel broadband orange-yellow-emitting phosphor for blue light-excited warm white LEDs. *ACS Appl. Mater. Interfaces* **2015**, *7*, 25219–25226. [[CrossRef](#)] [[PubMed](#)]
3. Mi, X.; Sun, J.; Song, D.; Shang, M.; Zhou, P.; Li, K.; Lin, J. Tunable luminescence and energy transfer properties in $\text{Ca}_8\text{MgLu}(\text{PO}_4)_7:\text{Ce}^{3+}, \text{Tb}^{3+}, \text{Mn}^{2+}$ phosphors. *J. Mater. Chem. C* **2015**, *3*, 4471–4481. [[CrossRef](#)]
4. Li, K.; Shang, M.; Zhang, Y.; Fan, J.; Lian, H.; Lin, J. Photoluminescence properties of single-component white-emitting $\text{Ca}_9\text{Bi}(\text{PO}_4)_7:\text{Ce}^{3+}, \text{Tb}^{3+}, \text{Mn}^{2+}$ phosphors for UV LEDs. *J. Mater. Chem. C* **2015**, *3*, 7096–7104. [[CrossRef](#)]
5. Liang, S.; Dang, P.; Li, G.; Molokeev, M.S.; Wei, Y.; Lian, H.; Shang, M.; Al-Kheraif, A.A.; Lin, J. Controllable two-dimensional luminescence tuning in $\text{Eu}^{2+}, \text{Mn}^{2+}$ doped $(\text{Ca}, \text{Sr})_9\text{Sc}(\text{PO}_4)_7$ based on crystal field regulation and energy transfer. *J. Mater. Chem. C* **2018**, *6*, 6714–6725. [[CrossRef](#)]
6. Chen, Y.; Li, Y.; Wang, J.; Wu, M.; Wang, C. Color-tunable phosphor of Eu^{2+} and Mn^{2+} codoped $\text{Ca}_2\text{Sr}(\text{PO}_4)_2$ for UV light-emitting diodes. *J. Phys. Chem. C* **2014**, *118*, 12494–12499. [[CrossRef](#)]
7. Huang, C.-H.; Wu, P.-J.; Lee, J.-F.; Chen, T.-M. $(\text{Ca}, \text{Mg}, \text{Sr})_9\text{Y}(\text{PO}_4)_7:\text{Eu}^{2+}, \text{Mn}^{2+}$: Phosphors for white-light near-UV LEDs through crystal field tuning and energy transfer. *J. Mater. Chem.* **2011**, *21*, 10489. [[CrossRef](#)]
8. Wang, C.; Wang, Z.; Li, P.; Cheng, J.; Li, Z.; Tian, M.; Sun, Y.; Yang, Z. Relationships between luminescence properties and polyhedron distortion in $\text{Ca}_{9-x-y-z}\text{Mg}_x\text{Sr}_y\text{Ba}_z\text{Ce}(\text{PO}_4)_7:\text{Eu}^{2+}, \text{Mn}^{2+}$. *J. Mater. Chem. C* **2017**, *5*, 10839–10846. [[CrossRef](#)]
9. Zhang, X.; Xu, J.; Guo, Z.; Gong, M. Luminescence and energy transfer of dual-emitting solid solution phosphors $(\text{Ca}, \text{Sr})_{10}\text{Li}(\text{PO}_4)_7:\text{Ce}^{3+}, \text{Mn}^{2+}$ for ratiometric temperature sensing. *Ind. Eng. Chem. Res.* **2017**, *56*, 890–898. [[CrossRef](#)]
10. Lv, Y.; Jin, Y.; Wu, H.; Liu, D.; Xiong, G.; Ju, G.; Chen, L.; Hu, Y. An all-optical ratiometric thermometer based on reverse thermal response from interplay among diverse emission centers and traps with high-temperature sensitivity. *Ind. Eng. Chem. Res.* **2019**, *58*, 21242–21251. [[CrossRef](#)]
11. Pasiński, D.; Sokolnicki, J. Broadband orange phosphor by energy transfer between Ce^{3+} and Mn^{2+} in $\text{Ca}_3\text{Al}_2\text{Ge}_3\text{O}_{12}$ garnet host. *J. Alloys Compd.* **2019**, *786*, 808–816. [[CrossRef](#)]
12. Dong, R.; Liu, W.; Song, Y.; Zhang, X.; An, Z.; Zhou, X.; Zheng, K.; Sheng, Y.; Shi, Z.; Zou, H. A promising single-phase, color-tunable phosphor $(\text{Ba}_{0.9}\text{Sr}_{0.1})_9\text{Lu}_2\text{Si}_6\text{O}_{24}:\text{Eu}^{2+}, \text{Mn}^{2+}$ for near-ultraviolet white-light-emitting diodes. *J. Lumin.* **2019**, *214*, 116585. [[CrossRef](#)]
13. Yan, J.; Zhang, Z.; Wen, D.; Zhou, J.; Xu, Y.; Li, J.; Ma, C.-G.; Shi, J.; Wu, M. Crystal structure and photoluminescence tuning of novel single-phase $\text{Ca}_8\text{ZnLu}(\text{PO}_4)_7:\text{Eu}^{2+}, \text{Mn}^{2+}$ phosphors for near-UV converted white light-emitting diodes. *J. Mater. Chem. C* **2019**, *7*, 8374–8382. [[CrossRef](#)]
14. Huang, C.-H.; Kuo, T.-W.; Chen, T.-M. Novel red-emitting phosphor $\text{Ca}_9\text{Y}(\text{PO}_4)_7:\text{Ce}^{3+}, \text{Mn}^{2+}$ with energy transfer for fluorescent lamp application. *ACS Appl. Mater. Interfaces* **2010**, *2*, 1395–1399. [[CrossRef](#)]
15. Liu, S.; Liang, Y.; Li, H.; Zhang, W.; Tu, D.; Chen, Y. Color tuning of $\beta\text{-Ca}_3(\text{PO}_4)_2$ -type phosphor with enhanced quantum efficiency via self-charge compensation for healthy and warm solid state lighting application. *Chem. Eng. J.* **2020**, *390*, 124463. [[CrossRef](#)]
16. Wang, C.; Li, P.; Wang, Z.; Sun, Y.; Cheng, J.; Li, Z.; Tian, M.; Yang, Z. Crystal structure, luminescence properties, energy transfer and thermal properties of a novel color-tunable, white light-emitting phosphor $\text{Ca}_{9-x-y}\text{Ce}(\text{PO}_4)_7:x\text{Eu}^{2+}, y\text{Mn}^{2+}$. *Phys. Chem. Chem. Phys.* **2016**, *18*, 28661–28673. [[CrossRef](#)]
17. Carrasco, I.; Piccinelli, F.; Bettinelli, M. Optical spectroscopy of $\text{Ca}_9\text{Tb}_{1-x}\text{Eu}_x(\text{PO}_4)_7$ ($x = 0, 0.1, 1$): Weak donor energy migration in the whitlockite structure. *J. Phys. Chem. C* **2017**, *121*, 16943–16950. [[CrossRef](#)]
18. Tong, X.; Han, J.; Zhang, X. Realization of color tunable via energy transfer in $\text{Ba}_{1.2}\text{Ca}_{0.8}\text{SiO}_4:\text{Tb}^{3+}$ phosphor. *J. Lumin.* **2019**, *216*, 116742. [[CrossRef](#)]
19. Bessière, A.; Benhamou, R.A.; Wallez, G.; Lecointre, A.; Viana, B. Site occupancy and mechanisms of thermally stimulated luminescence in $\text{Ca}_9\text{Ln}(\text{PO}_4)_7$ (Ln = lanthanide). *Acta Mater.* **2012**, *60*, 6641–6649. [[CrossRef](#)]
20. Ju, X.; Li, X.; Li, W.; Yang, W.; Tao, C. Luminescence properties of $\text{ZnMoO}_4:\text{Tb}^{3+}$ green phosphor prepared via co-precipitation. *Mater. Lett.* **2011**, *65*, 2642–2644. [[CrossRef](#)]

21. Reddy, G.L.; Moorthy, L.R.; Chengaiah, T.; Jamalaiah, B. Multi-color emission tunability and energy transfer studies of $\text{YAl}_3(\text{BO}_3)_4:\text{Eu}^{3+}/\text{Tb}^{3+}$ phosphors. *Ceram. Int.* **2014**, *40*, 3399–3410. [[CrossRef](#)]
22. Chung, H.-Y.; Lu, C.-H.; Hsu, C.-H. Preparation and photoluminescence properties of novel color-tunable $\text{MgY}_4\text{Si}_3\text{O}_{13}:\text{Ce}^{3+}, \text{Tb}^{3+}$ phosphors for ultraviolet light-emitting diodes. *J. Am. Ceram. Soc.* **2010**, *93*, 1838–1841. [[CrossRef](#)]
23. Chen, X.; Dai, P.; Zhang, X.; Li, C.; Lu, S.; Wang, X.; Jia, Y.; Liu, Y. A Highly efficient white light ($\text{Sr}_3\text{CaBa}(\text{PO}_4)_3\text{Cl}:\text{Eu}^{2+}, \text{Tb}^{3+}, \text{Mn}^{2+}$ phosphor via dual energy transfers for white light-emitting diodes. *Inorg. Chem.* **2014**, *53*, 3441–3448. [[CrossRef](#)] [[PubMed](#)]
24. Vijayalakshmi, L.; Kumar, K.N.; Hwang, P. Tailoring ultraviolet-green to white light via energy transfer from $\text{Tb}^{3+}\text{-Eu}^{3+}$ codoped glasses for white light-emitting diodes. *Scr. Mater.* **2020**, *187*, 97–102. [[CrossRef](#)]
25. Zhang, L.; Wang, Z.J.; Liu, C.J.; Dong, G.Y.; Dai, D.J.; Xing, Z.H.; Li, X.T.; Yang, Z.P.; Li, P.L. Tunable emitting phosphor $\text{Ca}_6\text{Ce}_2\text{Na}_2(\text{PO}_4)_6\text{F}_2:\text{Mn}^{2+}/\text{Tb}^{3+}$ for white LEDs: Luminescence, energy transfer and high thermal property. *J. Lumin.* **2020**, *217*, 116817. [[CrossRef](#)]
26. Dai, P.P.; Ma, R. Realizing efficient Mn^{2+} red emission via synergistic sensitization of Eu^{2+} and Tb^{3+} for white light-emitting diodes. *J. Alloys Compd.* **2020**, *812*, 152143. [[CrossRef](#)]
27. Zhang, Y.; Zhang, X.; Zhang, H.; Wu, Z.-C.; Liu, Y.; Ma, L.; Wang, X.; Liu, W.-R.; Lei, B. Enhanced absorption of $\text{Sr}_3\text{Lu}_2(\text{BO}_3)_4:\text{Ce}^{3+}, \text{Tb}^{3+}$ phosphor with energy transfer for UV-pumped white LEDs. *J. Alloys Compd.* **2019**, *789*, 215–220. [[CrossRef](#)]
28. Ye, S.; Zhang, J.; Zhang, X.; Lu, S.; Ren, X.; Wang, X.-J. Mn^{2+} concentration manipulated red emission in $\text{BaMg}_2\text{Si}_2\text{O}_7:\text{Eu}^{2+}, \text{Mn}^{2+}$. *J. Appl. Phys.* **2007**, *101*, 033513. [[CrossRef](#)]
29. Martín-Rodríguez, R.; Valiente, R.; Rodríguez, F.; Piccinelli, F.; Speghini, A.; Bettinelli, M. Temperature dependence and temporal dynamics of Mn^{2+} upconversion luminescence sensitized by Yb^{3+} in codoped $\text{LaMgAl}_{11}\text{O}_{19}$. *Phys. Rev. B* **2010**, *82*, 075117. [[CrossRef](#)]
30. Blasse, G. Energy transfer in oxidic phosphors. *Phys. Lett. A* **1968**, *28*, 444–445. [[CrossRef](#)]
31. Dexter, D.L.; Schulman, J.H. Theory of concentration quenching in inorganic phosphors. *J. Chem. Phys.* **1954**, *22*, 1063. [[CrossRef](#)]
32. Zhang, X.; Zhu, Z.; Guo, Z.; Sun, Z.; Yang, Z.; Zhang, T.; Zhang, J.; Wu, Z.-C.; Wang, Z. Dopant preferential site occupation and high efficiency white emission in $\text{K}_2\text{BaCa}(\text{PO}_4)_2:\text{Eu}^{2+}, \text{Mn}^{2+}$ phosphors for high quality white LED applications. *Inorg. Chem. Front.* **2019**, *6*, 1289–1298. [[CrossRef](#)]
33. Wang, B.; Kong, Y.; Chen, Z.; Li, X.; Wang, S.; Zeng, Q. Thermal stability and photoluminescence of Mn^{2+} activated green-emitting feldspar phosphor $\text{SrAl}_2\text{Si}_2\text{O}_8:\text{Mn}^{2+}$ for wide gamut w-LED backlight. *Opt. Mater.* **2020**, *99*, 109535. [[CrossRef](#)]
34. Lu, W.; Zhang, X.; Wang, Y.; Hao, Z.; Liu, Y.; Luo, Y.; Wang, X.; Zhang, J.; Liu, Y. Luminescence investigation and thermal stability study of Eu^{2+} and $\text{Eu}^{2+}\text{-Mn}^{2+}$ codoped $(\text{Ba,Sr})\text{Mg}_2\text{Al}_6\text{Si}_9\text{O}_{30}$ phosphor. *J. Alloys Compd.* **2012**, *513*, 430–435. [[CrossRef](#)]
35. Chen, D.; Liu, S.; Zhou, Y.; Wan, Z.; Huang, P.; Ji, Z. Dual-activator luminescence of $\text{RE/TM}:\text{Y}_3\text{Al}_5\text{O}_{12}$ ($\text{RE} = \text{Eu}^{3+}, \text{Tb}^{3+}, \text{Dy}^{3+}$; $\text{TM} = \text{Mn}^{4+}, \text{Cr}^{3+}$) phosphors for self-referencing optical thermometry. *J. Mater. Chem. C* **2016**, *4*, 9044–9051. [[CrossRef](#)]
36. Wang, X.; Zhao, Z.; Wu, Q.; Wang, C.; Wang, Q.; Yanyan, L.; Wang, Y. Structure, photoluminescence and abnormal thermal quenching behavior of Eu^{2+} -doped $\text{Na}_3\text{Sc}_2(\text{PO}_4)_3$: A novel blue-emitting phosphor for n-UV LEDs. *J. Mater. Chem. C* **2016**, *4*, 8795–8801. [[CrossRef](#)]

